Croatian Society for Materials Protection

*Metalurgija/Metallurgy*

**Vol. 65 No. 4 / 2026**

# Study on Surface Electromyography Electrode Based on MXene/PEDOT:PSS/PAAm Composite Material

**Liwen Chen [1,*], Weiying Wu [1], Bingyan Cui [1], Xintao Zhang [1], Jianyi Li [1], and Lei Guo [2]**

https://doi.org/10.64486/m.65.4.9

[1] College of Mechanical Engineering, North China University of Science and Technology, Tangshan 063000, China
[2] North China University of Science and Technology Affiliated Hospital , Tangshan 063000, China
* Correspondence: chenliwen@ncst.edu.cn

***Type of the Paper:*** Article
***Received:*** December 9, 2025
***Accepted:*** March 31, 2026

**Abstract:** Surface electromyography (sEMG) electrodes are critical components for signal acquisition; their material properties directly dictate the stability and accuracy of the recorded signals. To address the limitations of traditional electrodes, such as poor flexibility and signal interference, this study prepared a gel electrode based on MXene/PEDOT:PSS/PAAm. Key properties, including conductivity, adhesion, and stretchability, were systematically analyzed. Results indicate that an optimal PEDOT:PSS to MXene ratio of 6:4 yields a composite conductive material with a sheet resistance as low as 10.3 Ω/sq. Performance tests demonstrated that the electrode's adhesion strength to porcine skin tissue reached (49.10 ± 1.25) kPa. Furthermore, its contact impedance with human skin was significantly lower than that of standard Ag/AgCl electrodes in the (0.1–1000) Hz frequency range. In sEMG acquisition experiments, compared to Ag/AgCl electrodes, the prepared electrode exhibited a higher signal-to-noise ratio (SNR), lower root mean square error (RMSE), a smoother signal waveform, and a more stable baseline. The electrode demonstrates excellent conductivity and adhesion, providing a high-performance solution for wearable sEMG monitoring equipment.

**Keywords:** surface electromyography electrode; PEDOT:PSS; MXene; signal acquisition quality

## 1. Introduction

Surface electromyography (sEMG), an electrophysiological signal generated during muscle contraction, serves as a vital basis for evaluating muscle function, assisting in disease diagnosis, and optimizing motor performance. Generated prior to limb movement, sEMG offers the advantages of non-invasive measurement and rich information content, making it widely applicable in clinical medicine, rehabilitation engineering, and human-computer interaction [1,2].

As the core component for sEMG signal acquisition, electrodes strongly influence signal stability and accuracy. This performance depends on electrode–skin adhesion, biocompatibility, and electrical properties. However, most existing surface electromyography electrodes do not match the Young's modulus of human tissue, and their material properties are inadequate, resulting in insufficient matching of mechanical, electrical and biological properties between electrodes and human tissues, which is prone to tissue damage, electrode dislocation, motion artifacts and other problems. The traditional surface electromyography electrode is represented by Ag/AgCl wet electrode. Although it has the basic signal acquisition ability, it has many limitations: poor flexibility and difficulty in adapting to the dynamic deformation of the skin; long-term use is prone to

causing skin irritation, and the water volatilization of conductive gel leads to signal attenuation; most of them are single-use, high cost and lack of environmental protection [3,4].

In recent years, flexible electrodes have received extensive attention due to their good adhesion, biocompatibility and stretchability. Among them, conductive polymer hydrogels based on poly (3,4-ethylenedioxythiophene): polystyrene sulfonic acid (PEDOT:PSS) have become one of the ideal surface muscle electrode materials due to their ion-electron double conductivity, excellent biocompatibility, soft stretchability, Young 's modulus similar to tissues, convenient processing and manufacturing, and stability in physiological environment [5-7]. Xin Zhou et al. [8] prepared a thin film electrode by mixing PEDOT:PSS, ethylene glycol (EG) and tannic acid (TA). Meili Xia et al. [9] developed a compliant skin dry electrode with low interface impedance by encapsulating ultrathin paper-cut PEDOT:PSS/polyvinyl alcohol (PVA)/silver nanowires (Ag NWs) film. The contact impedance is about 27.41 kΩ at 100 Hz. In addition to conductive polymers, two-dimensional conductive materials have also attracted considerable interest in flexible electrode applications. MXenes are a family of two-dimensional transition metal carbides/nitrides derived from layered MAX phases through selective etching of the A-layer. The precursor MAX phases can be generally described by the formula $M_{n+1}AX_n$, where A is a group III or IV element, M is an early transition metal (such as Ti, Zr, V, and Mo), and X represents C or N [10,11]. During the synthesis process, MXenes typically undergo etching and delamination, accompanied by the introduction of surface terminations (Tx), which renders their interfacial chemistry and electrical properties tunable. Since MXenes were first reported in 2011, they have become a research hotspot in materials science due to their excellent electrical and thermal properties [12,13]. $Ti_3C_2Tx$, one of the most widely studied MXenes, usually exhibits high electrical conductivity, large specific surface area, and abundant surface functional groups, enabling efficient electron transport and improved charge transfer at the electrode–skin interface. As a result, the contact impedance can be reduced and the signal acquisition quality can be enhanced [14]. Owing to their high conductivity, favorable mechanical properties, and hydrophilicity, MXenes also show promising potential in flexible sensors [15]. For example, Wang et al. successfully constructed a self-powered electronic skin sensor by incorporating MXene nanosheets into a glycerol/poly(dimethylsiloxane) composite film. The sensor could adhere to the skin surface and stably monitor temperature variations from 15 °C to 25 °C, demonstrating good sensitivity and signal stability [16].

However, MXenes are prone to oxidative degradation in air and aqueous environments, which may damage their layered structure and cause a gradual decline in electrical conductivity, thereby limiting their long-term stability and reliability in practical applications. Therefore, designing MXene-based composites to stabilize the conductive network is an effective approach for advancing their application in flexible electrodes. In this context, combining MXene with PEDOT:PSS is considered an efficient strategy to optimize electrical and mechanical properties. On the one hand, MXene nanosheets serve as highly conductive fillers to construct low-impedance electron transport pathways; on the other hand, PEDOT:PSS promotes the dispersion of MXene sheets and provides interfacial bridging, which reduces inter-sheet contact resistance and improves the continuity of the conductive network, thus achieving both high conductivity and flexibility. In addition, introducing a flexible hydrogel network can further enhance skin-like mechanical compliance and interfacial adhesion, reducing motion-induced noise and mitigating motion artifacts. Luan, Zhang et al. incorporated MXene nanosheets into polyacrylamide (PAAm) and sodium alginate (SA) hydrogel networks via in situ polymerization to obtain multifunctional hydrogels with good tensile properties, which were capable of monitoring subtle potential variations [17]. Overall, by rationally designing the composition ratio and interfacial structure of the composite system, synergistic regulation of electrical conductivity, mechanical compatibility, and interfacial stability can be achieved, meeting the requirements of flexible functional electrodes for multi-performance integration.

In this study, based on PEDOT:PSS and MXene, the gel electrode was prepared by combining polydopamine nanoparticles (PDA ) and polyacrylamide (PAAm). The properties of the prepared materials were systematically analyzed, and the signal quality was compared with the traditional Ag/AgCl electrodes through the sEMG signal acquisition experiment, which provided a reference for the design and application of high-performance surface sEMG electrodes.


https://doi.org/10.64486/m.65.4.9

## 2. Materials and Methods

### *2.1 Experimental materials*

The primary materials used in this study include titanium aluminum carbide (50 g), lithium fluoride, hydrochloric acid (36 %~38 %), PEDOT:PSS, dopamine, NaOH (≥ 96 %), H2O2 (≥ 30 %), acrylamide (100 g), and ammonium persulfate.

### *2.2 Preparation of MXene*

The initial reaction solution was formed by mixing 15 mL concentrated hydrochloric acid with 5 mL deionized water at a temperature of 35 °C and a stirring speed of 550 rpm. Subsequently, 1.6 g LiF was slowly added and reacted for 5 min, and then 1 g $Ti_3AlC_2$ was gradually added. At this time, the reaction proceeded vigorously, and the addition speed needed to be carefully controlled to ensure safety. The whole reaction was carried out in a sealed container for about 35 h to ensure sufficient reaction. After the completion of the reaction, the pH value of the solution was gradually adjusted to 7 by multiple centrifugation and washing to obtain the MXene dispersion. The MXene dispersion was further ultrasonically treated in nitrogen-protected ice water for 2 h to obtain a multi-layer MXene sheet structure. In order to obtain single-layer/few-layer MXene, the obtained precipitate was added to deionized water and shaken well. The high-power ultrasonic machine was used for ultrasonication for 1 h, centrifugation at 10000 rpm, and repeated ultrasonic centrifugation for 10 min to obtain the supernatant to obtain a few-layer/single-layer MXene.

### *2.3 Preparation of PDA*

0.4 g DA-HCl was added to 10 mL (0.006 g/ mL) Tris-HCl and stirred for 6 hours to synthesize brown-black polydopamine (PDA). 3 mL 30 % H2O2 and 12 mL (0.012 g) were added and heated in an oil bath at 90 °C for 4 hours to synthesize PDA .

### *2.4 Preparation of MXene/PEDOT:PSS/PAAm gel electrode*

In order to obtain the best conductivity of the composite, PEDOT:PSS and MXene were mixed according to the preset different proportions, which were 100 % PEDOT:PSS, 90 % PEDOT:PSS/10 % MXene, 80 % PEDOT:PSS/20 % MXene, 70 % PEDOT:PSS/30 % MXene, 60 % PEDOT:PSS/40 % MXene and 50 % PEDOT:PSS/ 50 % MXene, respectively. After different proportions of conductive materials were prepared, magnetic stirring was performed for 2-3 h to obtain a mixed conductive material. For different proportions of conductive materials, a standardized curing process was used to solidify the conductive materials into a film, and the square resistance of the conductive materials with different mixing ratios was tested to evaluate the conductivity of the conductive materials.

0.02 g HPC was added to 3 mL aqueous solution of monolayer/few-layer MXene with different concentrations, stirred at room temperature for 30 min, and fully dissolved. 1.5 g AAm was added to the above solution and stirred at room temperature for 30 min. After AAm was completely dissolved, 300 μL PDA was added, 0.035 g APS was added as initiator, 15 μL TMEDA was used as curing catalyst, and 50 μL MBAA (0.025 g/ mL) was added as chemical crosslinking agent. After stirring at room temperature for 15 min, the mixed solution was poured into the mold and stood still. After waiting for 30 min at room temperature, polyacrylamide gel was formed by self-polymerization. After demoulding, MXene/PEDOT:PSS/PAAm gel electrode was obtained.

## 3. Results and discussion

### *3.1 Material performance test*

#### *3.1.1 Conductivity test*

In order to explore the optimal mixing ratio of MXene and PEDOT:PSS conductive materials, the conduc-


https://doi.org/10.64486/m.65.4.9

tive materials of different proportions of MXene and PEDOT:PSS were mixed in a petri dish for high temperature curing to prepare conductive material films with different mixing ratios. Subsequently, these films were characterized by square resistance test. Three samples of each film were selected for testing. Each sample was tested at nine evenly distributed positions, and the average value was calculated to determine the square resistance of conductive materials with different mixing ratios. The results are shown in Figure 1. From the diagram, it can be seen that with the increase of MXene content, the square resistance value shows a trend of decreasing first and then increasing. When the proportion of MXene reaches 40 %, the square resistance value decreases to the lowest 10.3 Ω/sq. Considering that MXene is easy to oxidize, which in turn affects the conductivity, we believe that the use of a lower MXene content of the mixed material is more conducive to improving the stability of the material while maintaining the conductivity. Based on this result, a mixed conductive material containing 40 % MXene (i.e., PEDOT:PSS/MXene ratio of 6:4) was selected for subsequent experiments.

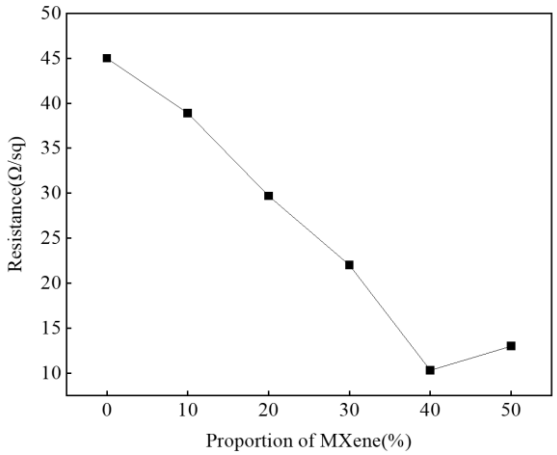


**Figure 1.** Effect of different proportions of MXene content on the surface sheet resistance of conductive materials

3.1.2 Adhesion and tensile test

Excellent adhesion is one of the core prerequisites for accurate recording of electrophysiological signals. It can not only ensure stable contact between the electrode and the interface, but also reduce signal distortion under motion [18,19]. As shown in Figure 2, the prepared MXene/PEDOT:PSS/PAAm hydrogel exhibits strong adhesion to biological tissues (e.g., porcine skin and muscle) as well as to common engineering substrates, including glass, plastic, wood, and metal. This excellent interfacial bonding force is mainly due to the synergistic interaction between the abundant functional groups in the hydrogel matrix and the substrate surface, including the widespread hydrogen bonding and electrostatic interactions, as well as the π-π stacking, cation-π interactions and metal coordination bonds derived from the conductive components.

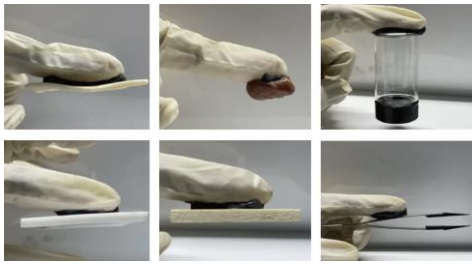

**Figure 2.** Hydrogels attached to different substrates


https://doi.org/10.64486/m.65.4.9

In order to quantitatively evaluate the adhesion strength of the hydrogel, the standard lap shear test was used for experimental determination. For each substrate, 10 independent measurements were performed under identical conditions, and the average value was calculated. Figure 3 shows the adhesion strength between the electrode gel and different substrates, The error bars represent the standard deviation of the measured values. From the figure, it can be seen that the adhesion strength of hydrogel and biomaterials is higher than that of engineering solid materials. The adhesion strength of porcine skin tissue is the highest, reaching 49.10 ± 1.25 kPa. In addition, the prepared electrode gel can still maintain stable conformal contact with the skin under dynamic deformation such as finger bending, and no obvious peeling or slippage occurs, as shown in Figure 4. The MXene/PEDOT:PSS/PAAm gel electrode has excellent static adhesion strength and dynamic adhesion stability. It can maintain compliance contact with tissues at complex interfaces and motion states, prevent peeling/stretching, and effectively avoid sEMG signal interference caused by electrode shedding or relative displacement, which provides a key guarantee for long-term acquisition of high-quality electrophysiological signals.

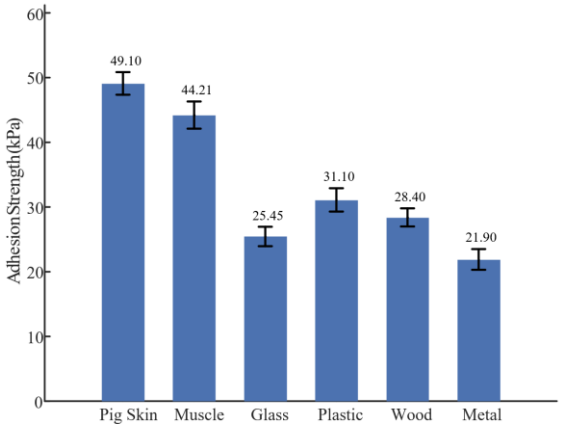


**Figure 3.** Adhesion strength between electrode gel and different substrates

**Figure 4.** Adhesion effect at different angles

3.1.3 Electrode-skin contact impedance test

The magnitude of the contact impedance is an important criterion to measure the quality of bioelectrical signals. Therefore, the quality of the electrode can be preliminarily judged by the strength of the collected contact impedance signal. Clinically, the traditional Ag/AgCl electrodes are widely used for bioelectrical signal monitoring. When the electrode contact impedance is similar to the Ag/AgCl electrodes or smaller than the Ag/AgCl electrodes, the current can be transmitted more effectively and the background noise is lower. The resistance of the human body surface will change due to changes in temperature, humidity, and thickness of the skin stratum corneum. Therefore, it is not reliable to use different time periods as a comparison. The common comparison method is to continuously measure the contact impedance between the prepared electrode and the Ag/AgCl electrodes. The unsolidified hydrogel was filled into a silica gel mold with a diameter of 1.5 cm and a depth of 5 mm to make a MXene/PEDOT:PSS/PAAm electrode. By fixing two Ag/AgCl electrodes and one test electrode on the inside of the subject's wrist, the distance of each electrode is 2cm for the electrode-skin contact impedance test.


https://doi.org/10.64486/m.65.4.9

Before fixing the electrode, the skin on the inside of the wrist was treated with alcohol cotton. The signal voltage of the contact impedance measurement is set to 5 mV, and the frequency range of the test signal is 0.1–1000 Hz. To ensure data consistency and minimize variability caused by individual skin differences, the baseline contact impedance measurement was conducted on a single healthy male subject. Each measurement was repeated five times at each frequency, and the average value was obtained for comparison. It can be seen from Figure 5 that the contact impedance of the MXene/PEDOT:PSS/PAAm gel electrode in the frequency range of 0.1–1000 Hz is smaller than that of the Ag/AgCl electrodes, which means that the electrode gel prepared in this paper has greater advantages in recording bioelectrical signals.

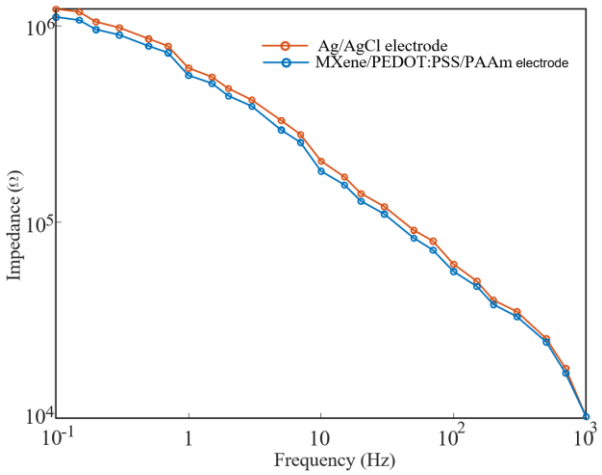


**Figure 5.** Contact impedance comparison between the MXene/PEDOT:PSS/PAAm gel electrode and the Ag/AgCl electrodes

*3.2 sEMG signal acquisition test*

In order to test the reliability and stability of the prepared electrode in the actual acquisition of sEMG, the performance of the traditional Ag/AgCl electrodes was compared, and the sEMG signal acquisition experiment was carried out using the Delsys sEMG signal acquisition instrument (sampling frequency is set to 1000 Hz). Signal-to-Noise Ratio (SNR) and Root Mean Square Error (RMSE) were introduced as evaluation indexes [20,21]. The mean value of the same muscle of each subject was calculated to evaluate the signal acquisition quality and anti-interference ability of the electrode.

$$SNR = 10\log_{10}\left(\frac{\sum_{i=1}^{N} x(i)^2}{\sum_{i=1}^{N}(x(i)-f'(i))^2}\right) \quad (1)$$

$$RMSE = \sqrt{\frac{1}{N}\sum_{i=1}^{N}(x(i)-f'(i))^2} \quad (2)$$

Where $x(i)$ is the original signal, $f'(i)$ is the denoised signal, and $N$ is the signal length. SNR reflects the enhancement of signal quality after denoising, while RMSE quantifies the deviation between the original and processed signals. The larger the SNR and the smaller the RMSE, the better the denoising effect.

To evaluate the performance of the electrode in practical sEMG signal acquisition and to assess its applicability and stability across different individuals, eight healthy volunteers (4 males and 4 females) were recruited, aged (22–28) years, with a height range of (165–182) cm and a weight range of (52–75) kg. All subjects had no history of musculoskeletal diseases, skin inflammation or allergies, did not perform high-intensity exercise before the experiment, and signed informed consent to clarify the experimental process and precautions. During the experiment, each subject performed elbow flexion and extension movements. Each

 https://doi.org/10.64486/m.65.4.9

movement lasted for 3 s and was repeated five times, with a 30 s rest interval between movements to avoid muscle fatigue. The prepared gel electrode and the conventional Ag/AgCl electrode were attached to the biceps brachii and triceps brachii, respectively, and the sEMG signals were recorded simultaneously under identical conditions. Based on the acquired signal data, MATLAB software was used to process the signals obtained from the two types of electrodes, and SNR and RMSE were calculated. The time-domain sEMG signals recorded using the Ag/AgCl electrode and the MXene/PEDOT:PSS/PAAm gel electrode are shown in Figures 6 and 7, respectively, and the corresponding quantitative results are presented in Table 1.

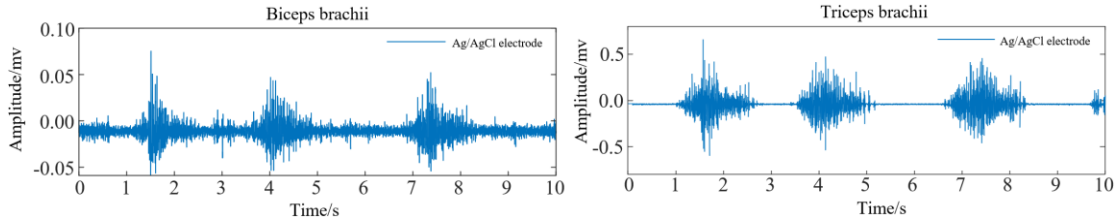


**Figure 6.** The sEMG signals were collected using Ag/AgCl electrodes

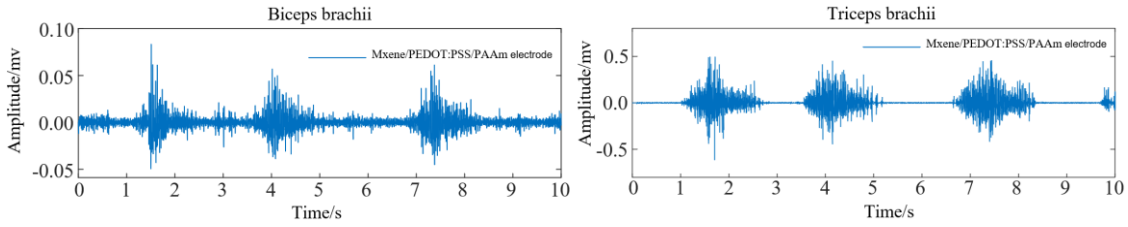


**Figure 7.** The sEMG signals were collected using MXene/PEDOT:PSS/PAAm electrodes

As shown in Figure 6 and 7, both electrodes can accurately capture the electrical signals associated with muscle contraction and relaxation. The signal peaks and troughs are clear, the characteristic peaks are clear and distinguishable, and the baseline is stable. Compared to the traditional Ag/AgCl signals, the waveforms collected by the composite gel electrode exhibited significantly fewer artifacts and a smoother profile, with a notable reduction in baseline drift. Electrodes can maintain relatively stable peaks, which represent the strength of muscle contraction and are important indicators for analyzing muscle function.

**Table 1.** Comparison of signal evaluation indices of two electrodes

| Electrode | Biceps brachii | | Triceps brachii | |
|---|---|---|---|---|
| | SNR | RMSE | SNR | RMSE |
| Ag/AgCl | 12.3 | 0.3214 | 13.1 | 0.2956 |
| MXene/PEDOT:PSS/PAAm | 15.4 | 0.1208 | 16.2 | 0.1147 |

According to the signal evaluation indices presented in Table 1, the average SNR values of MXene/PEDOT:PSS/PAAm gel electrode in biceps brachii and triceps brachii were 15.4 and 16.2, respectively, which were higher than 12.3 and 13.1 obtained by Ag/AgCl electrodes, and RMSE were 0.1208 and 0.1147, respectively, which were significantly lower than 0.3214 and 0.2956 of Ag/AgCl electrodes. The results show that the signal acquisition quality of the gel electrode is better, which is due to its low contact impedance, good skin adhesion and conformality, which can effectively reduce motion artifacts and ensure signal stability.


https://doi.org/10.64486/m.65.4.9

## 4. Conclusions

The MXene/PEDOT:PSS/PAAm composite gel electrode prepared in this study employs two-dimensional MXene, derived from MAX phases via selective etching, as the core conductive filler. Through a composite structural design with PEDOT:PSS, the electrode maintains the metal-like electrical conductivity of MXene while contributing to improved environmental stability and overall interfacial performance, thereby achieving a synergistic optimization of electrical and mechanical properties. Experimental results indicate that when the mixing ratio of PEDOT:PSS to MXene is 6:4, the electrode exhibits a low sheet resistance of 10.3 Ω/sq. Performance tests further demonstrate excellent interfacial conformability and adhesion, with an adhesion strength of 49.10 ± 1.25 kPa to porcine skin. In addition, the contact impedance within the frequency range of 0.1–1000 Hz is lower than that of Ag/AgCl electrodes. sEMG signal acquisition experiments show that the gel electrode provides a higher signal-to-noise ratio and a lower root mean square error, producing smoother waveforms with reduced interference and enabling accurate capture of muscle contraction characteristics. Overall, the MXene/PEDOT:PSS/PAAm gel electrode exhibits excellent conductivity, adhesion, and promising skin-interface performance, delivering better signal acquisition quality than traditional Ag/AgCl electrodes and providing a high-performance solution for wearable sEMG monitoring devices.

Statement: All subjects involved in the study were fully informed of the experimental procedures and potential risks, and provided written informed consent prior to participation

Funding: Innovation and Entrepreneurship Education Teaching Reform Research and Practice Project of Hebei Province (2023cxcy095); Graduate Course Reform Project of Hebei Province (YKCSZ2022068);Innovation Team for the Theoretical Basis of Robot Kinematics in Tangshan City (21130208D); Basic Research Project of Tangshan City (23130201E); Key Scientific Research Project of North China University of Science and Technology (ZD-YG-202306); Professional Degree Comprehensive Reform Project of North China University of Science and Technology (ZD18010223); Key Scientific Re-search Project of North China University of Science and Technology (ZD-YG-JBGS202513)

## References

[1] Z. Y. Du, Y. D. Xu, A. Y. Cheng, et al., "Myoelectric fatigue and motor-unit firing patterns during sinusoidal vibration superimposed on low-intensity isometric contraction," *IEEE Transactions on Neural Systems and Rehabilitation Engineering*, vol. 32, pp. 3773-3781, 2024, https://doi.org/10.1109/TNSRE.2024.3471856

[2] C. J. Thomson, T. N. Tully, E. S. Stone, et al., "Enhancing neuroprosthesis calibration: the advantage of integrating prior training over exclusive use of new data," *Journal of Neural Engineering*, vol. 21, art. no. 066020, 2024, https://doi.org/10.1088/1741-2552/ad94a7

[3] S. Lobodzinski, U. Teppner, and M. Laks, "Biopotential fiber sensors have equivalent in vivo electric performance to standard Ag-AgCl wet electrodes," *Journal of Electrocardiology*, vol. 42, no. 6, pp. 616, 2009, https://doi.org/10.1016/j.jelectrocard.2009.08.034

[4] N. Larpant, A. D. Pham, A. Shafaat, et al., "Sensing by wireless reading Ag/AgCl redox conversion on RFID tag: universal, battery-less biosensor design," Scientific Reports, vol. 9, no. 1, pp. 12948, 2019, https://doi.org/10.1038/s41598-019-49245-3

[5] L. V. Kayser and D. J. Lipomi, "Stretchable conductive polymers and composites based on PEDOT and PEDOT:PSS," Advanced Materials, vol. 31, pp. 1806133, 2019, https://doi.org/10.1002/adma.201806133

[6] V. R. Feig, H. Tran, M. Lee, et al., "An electrochemical gelation method for patterning conductive PEDOT:PSS hydrogels," Advanced Materials, vol. 31, pp. 1902869, 2019, https://doi.org/10.1002/adma.201902869

[7] Z. Bian, Y. Li, H. Sun, et al., "Transparent, intrinsically stretchable cellulose nanofiber-mediated conductive hydrogel for strain and humidity sensing," *Carbohydrate Polymers*, vol. 301, art. no. 120300, 2023, https://doi.org/10.1016/j.carbpol.2022.120300

[8] X. Zhou, P. Kateb, J. Fan, et al., "Conducting polymer films and bioelectrodes combining high adhesion and electro-mechanical self-healing," Journal of Materials Chemistry C, vol. 12, no. 16, pp. 5708-5717, 2024, https://doi.org/10.1039/d3tc04230h

[9] M. Xia, J. Liu, B. J. Kim, et al., "Kirigami-Structured, Low-Impedance, and Skin-Conformal Electronics for Long-Term Biopotential Monitoring and Human–Machine Interfaces," Advanced Science, vol. 11, no. 1, pp. 2304871, 2024, https://doi.org/10.1002/advs.202304871

[10] R. S. Devan, R. A. Patil, J. H. Lin, et al., "One-dimensional metal-oxide nanostructures: recent developments in synthesis, characterization, and applications," Advanced Functional Materials, vol. 22, no. 16, pp. 3326-3370, 2012, https://doi.org/10.1002/adfm.201201008

[11] Z. M. Sun, "Progress in research and development on MAX phases: a family of layered ternary compounds," International Materials Reviews, vol. 56, no. 3, pp. 143-166, 2011. https://doi.org/10.1179/1743280410Y.0000000001.

[12] B. Anasori and M. Naguib, eds., "Two-dimensional MXenes," MRS Bulletin, vol. 48, no. 3, pp. 238-244, 2023, https://doi.org/10.1557/s43577-023-00500-z

[13] J. Zhang, X. Wang, G. Hang, et al., "Recent advances in MXene-based fibers, yarns, and fabrics for wearable energy storage devices applications," ACS Applied Electronic Materials, vol. 5, no. 9, pp. 4704-4725, 2023, https://doi.org/10.1021/acsaelm.3c00238

[14] M. Naguib, M. Kurtoglu, V. Presser, et al., "Two-dimensional nanocrystals produced by exfoliation of $Ti_3AlC_2$," in MXenes. Jenny Stanford Publishing, 2023, pp. 15-29.

[15] X. Wang, Y. Tao, S. Pan, et al., "Biocompatible and breathable healthcare electronics with sensing performances and photothermal antibacterial effect for motion-detecting," npj Flexible Electronics, vol. 6, no. 1, pp. 1-15, 2022, https://doi.org/10.1038/s41528-022-00228-x

[16] M. M. Wang, W. Q. Liu, X. Shi, et al., "Self-powered and low-temperature resistant MXene-modified electronic-skin for multifunctional sensing," Chemical Communications, vol. 57, no. 70, pp. 8790-8793, 2021, https://doi.org/10.1039/D1CC02211C

[17] H. Luan, D. Zhang, Z. Xu, et al., "MXene-based composite double-network multifunctional hydrogels as highly sensitive strain sensors," Journal of Materials Chemistry C, vol. 10, no. 19, pp. 7604-7613, 2022, https://doi.org/10.1039/D2TC00679K

[18] H. Pang, H. Liu, Q. Yan, J. Li, C. Ma, and S. Zhang, "A tough, adhesive, self-healable, and antibacterial plant-inspired hydrogel based on pyrogallol borax dynamic cross-linking," Journal of Materials Chemistry B, vol. 9, pp. 4230-4240, 2021, https://doi.org/10.1039/D1TB00763G

[19] D. Gan, W. Xing, L. Jiang, J. Fang, C. Zhao, F. Ren, L. Fang, K. Wang, and X. Lu, "Plant-inspired adhesive and tough hydrogel based on Ag-lignin nanoparticles-triggered dynamic redox catechol chemistry," Nature Communications, vol. 10, pp. 1487, 2019, https://doi.org/10.1038/s41467-019-09351-2

[20] P. K. Koppolu and K. Chemmangat, "Automatic selection of IMFs to denoise the sEMG signals using EMD," Journal of Electromyography and Kinesiology, vol. 73, pp. 102834, 2023, https://doi.org/10.1016/j.jelekin.2023.102834

[21] F. Xiao, D. Yang, X. Guo, et al., "VMD-based denoising methods for surface electromyography signals," Journal of Neural Engineering, vol. 16, no. 5, pp. 056017, 2019, https://doi.org/10.1088/1741-2552/ab33e4